Supporting Online Material for

ER Tubules Mark Sites of Mitochondrial Division

Jonathan R. Friedman, Laura L. Lackner, Matthew West, Jared R. DiBenedetto, Jodi Nunnari, and Gia K. Voeltz*

*To whom correspondence should be addressed. Email: gia.voeltz@colorado.edu

This PDF file includes:

Other Supporting Online Material for this manuscript includes the following:

Materials and Methods

Yeast strains and plasmids

Strain W303 (*ade2–1*; *leu2–3*; *his3–11, 15*; *trp1–1*; *ura3–1*; *can1–100 MatA*) and NDY257 (BY4741 *his3Δ1 leu2Δ met15Δ ura3Δ rtn1::kanMX4 rtn2::kanMX4 yop1::kanMX4*) were described previously (*15, 20*). For EM analysis, wild type strain BY4742 (models c, d; (*14*)) or a strain expressing endogenous levels of Rtn1-GFP (models a, b; Invitrogen, (*15*)) was used. The plasmids pVT100U-dsRED (mito-dsRED), pYX223mitoCFP (mito-CFP), pHS20-mCherry (Dnm1-mCherry), pJK59 (Sec63-GFP), and YIplac204/TKC-GFP-HDEL (GFP-HDEL) were described previously (*20-23*). W303 GFP-HDEL was created by transforming W303 with EcoRV linearized YIplac204/TKC-GFP-HDEL. To construct pYX142-dsRed, GFP in pYX142-mtGFP was replaced with dsRED using standard cloning techniques (*24*).

Yeast cytological analysis

To visualize mitochondria and ER in WT cells, W303 GFP-HDEL was transformed with pVT100U-dsRED. To visualize mitochondria and ER in the absence of Rtns/Yop1, NDY257 was transformed with pJK59 and pYX142-dsRed. Before imaging, the WT and Rtns/Yop1 mutant strains were grown to log phase in SC-Ura + 2% dextrose or SC-Ura-Leu + 2% dextrose media, respectively. Cell monolayers were created by flowing cells into the imaging chamber of a CellAsic Y04C plate using an ONIX Microfluidic Perfusion Platform or by mounting cells on a 3% agarose pad. For both strains, Z-series of cells were imaged over time using the spinning disc module of a Marianas SDC Real Time 3D Confocal-TIRF microscope (Intelligent Imaging Innovations, 3i) fit with a 100x, 1.46 NA objective and EMCCD camera. A step size of 0.4 μm was used. Image capture and post-capture processing were done using SlideBook5 software (3i), and Photoshop (Adobe) was used to make linear adjustments to brightness and contrast. Interpolated images are shown.

To visualize Dnm1, mitochondria, and ER, W303 GFP-HDEL was co-transformed with pYX223mitoCFP and pHS20-mCherry. For imaging, cells were grown to log phase in SC-His-Leu + 2% galactose media, concentrated by centrifugation and mounted on a 3% agarose pad. Either single focal planes over time or whole cell z-series at a single time point were captured using a DeltaVision-Real Time microscope fit with a 60x, 1.4 NA objective and CoolSnap HQ camera. For the z-series, a step size of 0.2 μm was used. Image capture and post-capture processing were done using softWoRx software (Applied Precision), and Photoshop (Adobe) was used to make linear adjustments to brightness and contrast. Deconvolved images are shown.

Yeast electron microscopy

Cells were grown to mid-log phase, high pressure frozen, and processed for EM, tomography, and 3-D modeling as previously described (*14*). Tomograms were constructed and mitochondrial measurements were computed using IMOD (*25*) and its newest viewer, 3DMOD 4.0.11.

To determine the percentage of mitochondrial circumference in contact with the ER membrane, a 30 nm wide line, centered at the ER-mitochondrial contact, was drawn at ~10 nm intervals surrounding the surface of the mitochondrial membrane. ER contact with that line was determined if the ER membrane was within 30 nm of the line and ribosomes were excluded in the space between the line and the ER membrane. The percentage of those lines that were classified as positive for contact was used to calculate the percentage of mitochondrial circumference in contact with the ER, and is denoted as red objects in the 3-D models.

To determine the diameter of mitochondria at ER contacts, two perpendicular diameters of the mitochondrial cross-section were averaged at the center of the contact site. To determine the diameter of the mitochondrion extending away from the ER contact, diameters were measured in 50 nm intervals moving along a line drawn orthogonal to the cross section.

Mammalian plasmids and RNAi oligonucleotides

Mito-dsRed and mito-EGFP were gifts from D. Chan (California Institute of Technology), and described previously (*26*). GFP-Sec61β (*27*) and mCherry-KDEL (*28*) were previously described. BFP-KDEL was generated by PCR amplifying the coding sequence of TagBFP with primers containing the BiP ER signal sequence and the KDEL ER retention sequence, and replacing the existing TagBFP sequence of pTagBFP-C (Evrogen) using the NheI/KpnI sites. Mito-BFP was generated by first replacing the GFP sequence of pAcGFP1-N1 (Clontech) with TagBFP into the BamHI/NotI sites, and then cloning amino acids 1-22 of *S. cerevisiae* COX4 into the XhoI/BamHI sites of that vector. mCherry-Drp1 was generated by PCR amplifying human Drp1 isoform 3 (NCBI accession number NM_005690) and cloning it into the XhoI/BamHI sites of mCherry-α-tubulin (*13*), replacing α-tubulin. GFP-Mff was generated by PCR amplifying full length Mff (isoform 1; NCBI accession number NM_020194) and cloning it into the XhoI/BamHI sites of pAcGFP1-C1 (Clontech).

Oligonucleotides for Drp1 siRNA were synthesized by Qiagen (SI02661365) against the target sequence: 5'-CAGGAGCCAGCTAGATATTAA-3'. Oligonucleotides for Mff siRNA were synthesized by Qiagen against the target sequence: 5'-AACGCTGACCTGGAACAAGGA-3' (*18*). Oligonucleotides for Mfn2 siRNA were synthesized by Invitrogen (HSS115028) against the target sequence: 5'-GGACCTCCATGGGCATTCTTGTTGT-3' (*29*). As a control, Silencer Negative Control #1 siRNA (Ambion) was used.

Mammalian cell growth, transfection, and drug treatment

Cos-7 cells (ATCC) were grown in DMEM supplemented with 10% FBS and 1% penicillin/streptomycin. Cells were seeded at $2x10^5$ cells per well of a 6-well dish (or equivalent density) ~16 hours prior to transfection. Plasmid transfections were performed in OPTI-MEM media (Invitrogen) with 5 μL Lipofectamine 2000 (Invitrogen) per well for ~5 hours, followed by splitting to glass-bottom microscope dishes (MatTek) at a concentration of ~$0.8x10^5$ cells per mL. Cells were imaged in OPTI-MEM media ~16-24 hours after plating on microscope dishes. For all experiments, the following

amounts of DNA were transfected per well: 50 ng mito-dsRed; 50 ng mito-EGFP; 1 μg GFP-Sec61β; 0.5 μg mCherry-KDEL; 1 μg BFP-KDEL; 1 μg mito-BFP; 0.3 μg mCherry-Drp1; 0.1 μg GFP-Mff. RNAi transfections were performed as above, except with an additional transfection step; cells were seeded as above and transfected with 2.5 μL siLentFect (Bio-Rad) and 40 nM RNAi oligonucleotides, split 1:2 ~24 hours post-transfection, and re-transfected ~24 hours later with 5 μL Lipofectamine 2000, 40 nM RNAi oligonucleotides, and appropriate plasmid DNA. In the case of simultaneous Mfn2 and Drp1 RNAi, each oligonucleotide was treated at 40 nM. During drug treatment, cells were treated with 10 μM BAPTA-AM (Calbiochem) in OPTI-MEM media during imaging.

Mammalian cell confocal microscopy

Imaging of live cells was performed with an inverted fluorescence microscope (TE2000-U; Nikon) equipped with an electron-multiplying charge-coupled device camera (Cascade II; Photometrics) and a Yokogawa spinning disc confocal system (CSU-Xm2; Nikon). Images were taken with a 100x NA 1.4 oil objective and imaging was performed at 37°C. Images were acquired using MetaMorph (version 7.0; MDS Analytical Technologies) and contrasted and merged using Photoshop (Adobe), MetaMorph, or ImageJ (National Institutes of Health). Scale bars were generated using ImageJ.

Western blot

Whole cell lysates of Cos-7 cells were resuspended in Laemmli sample buffer, boiled 10 minutes, separated by SDS-PAGE, and transferred to a PVDF membrane. Primary antibodies to Drp1 (Dnm1L), Mff, and Mfn2 for Western blotting were purchased from Abcam, Proteintech, and Sigma-Aldrich, respectively. Antibody to GAPDH for Western blotting was purchased from Sigma-Aldrich. HRP-conjugated goat anti–rabbit or goat anti–mouse secondary antibodies (Sigma) were used, and signal was detected with SuperSignal West Pico Chemiluminescent solution (Thermo Fisher Scientific).

Drp1 association with ER-mitochondrial contacts

Cos-7 cells expressing markers for ER, mitochondria, and Drp1 were visualized live by confocal fluorescence microscopy every five seconds for two minutes in a single focal plane. Punctae were counted if they were in regions of the cell with resolvable ER tubules. By imaging Drp1 punctae over time, we could ensure that we were observing stable rather than transient Drp1 structures, and confirm whether they maintain interaction with the ER membrane during the course of the movie.

Mitochondrial division analysis in mammalian cells

To identify sites of mitochondrial division, Cos-7 cells expressing markers for the ER and mitochondria were imaged every 10 seconds for up to 30 minutes in a single focal plane. To determine the ER tubule coverage of mitochondria, we analyzed the image immediately preceding mitochondrial division for all events. We traced the outline of the mitochondrion using ImageJ, and made any included pixels a binary value of 1. We then traced any ER tubules that crossed the mitochondrion, omitting any ER tubules that ran parallel to the mitochondrion. The traced ER tubules were also given a binary value of 1, and this image was merged with the mitochondrial trace. To determine the percent of the

mitochondrial image covered by crossing ER tubules, we compared the number of pixels positive for ER signal to number of potential pixels from the mitochondria image.

Mitochondrial constrictions in mammalian cells

To identify mitochondrial constrictions, z-series were imaged in increments of 0.2 μm centered on the middle focal plane of the mitochondrial constriction. Constrictions were identified when present in multiple planes of the z-series and marked by Drp1 or Mff. In the case of Mff depletion, constrictions were identified only by an obvious fluorescence minimum in multiple focal planes. Linescans were performed using MetaMorph by drawing a line through the middle of the mitochondrion on the appropriate focal plane, and allowed us to compare the fluorescence of the ER, as well as Drp1 or Mff, to the fluorescence minimum at the mitochondrial constriction.

SOM Text

ER-mitochondrial contacts at constriction sites occur independently of Mfn2

In mammalian cells, Mfn2 plays a role in the formation of mitochondrial-ER contacts (*11*). To address a potential role of Mfn2 in ER-associated mitochondrial division, we depleted Mfn2 by siRNA and examined ER-mitochondrial contact sites (Fig. S7A-B) and ER-associated mitochondrial constriction sites as marked by Mff in Cos-7 cells depleted of Mfn2 and Drp1 (Fig. S7B-E). No significant changes were detected in the ability of Mff punctae to localize to positions of ER-mitochondrial contacts or ER-mediated mitochondrial constriction in cells lacking Mfn2. Thus, a yet to be identified tethering complex may mediate the interaction between the ER and mitochondria at mitochondrial division sites.

ER marks sites of Drp1-dependent mitochondrial division induced upon cytosolic Ca^{2+} depletion

In mammalian cells, ER-mitochondrial contacts function in Ca^{2+} signaling (*10*). We asked whether Drp1-dependent mitochondrial division is affected by depletion of cytosolic Ca^{2+} levels using the membrane-permeable chelator BAPTA-AM. BAPTA-AM treatment caused an increase in mitochondrial fragmentation that was the result of an increase in the frequency of ER-associated Drp1-dependent mitochondrial division events (97%, n=35; Fig. S8). Thus, ER tubules participate in mitochondrial division induced by disrupted Ca^{2+} levels.

Supplemental Figures

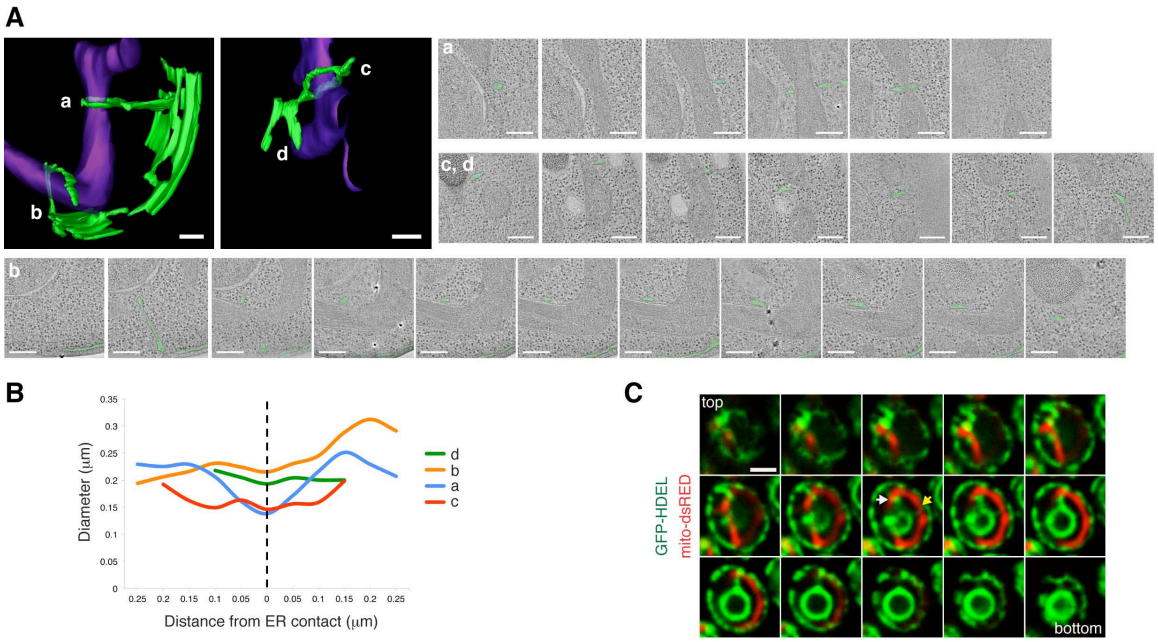

Figure S1. ER tubule-mediated constriction of mitochondria and division occurs at ER contacts in yeast cells. (A) 3-D model and the multiple EM tomographs in z-series of the contact sites between ER (drawn green) and mitochondria (as in Fig. 1). Lower-case letters on models correspond to the labels on the image series. Images shown are in (a) 40 nm, (b) 36 nm, and (c,d) 38 nm intervals in the z-plane. (B) To determine the relationship between ER contact and mitochondrial diameter, the diameter of mitochondria was measured in 50 nm intervals moving away from contact sites. Each line on graph corresponds to the letter shown on the model in (A). (C) A z-series showing ER tubules crossed over (yellow arrow) or wrapped around (white arrow) mitochondria at future mitochondrial division sites from the cell shown in Fig. 1B, at t=40 sec. Arrows are placed in the focal plane shown in Fig. 1B and indicate sites where mitochondrial division subsequently occurred. Scale bars: (A) 200 nm; (C) 2 μm.

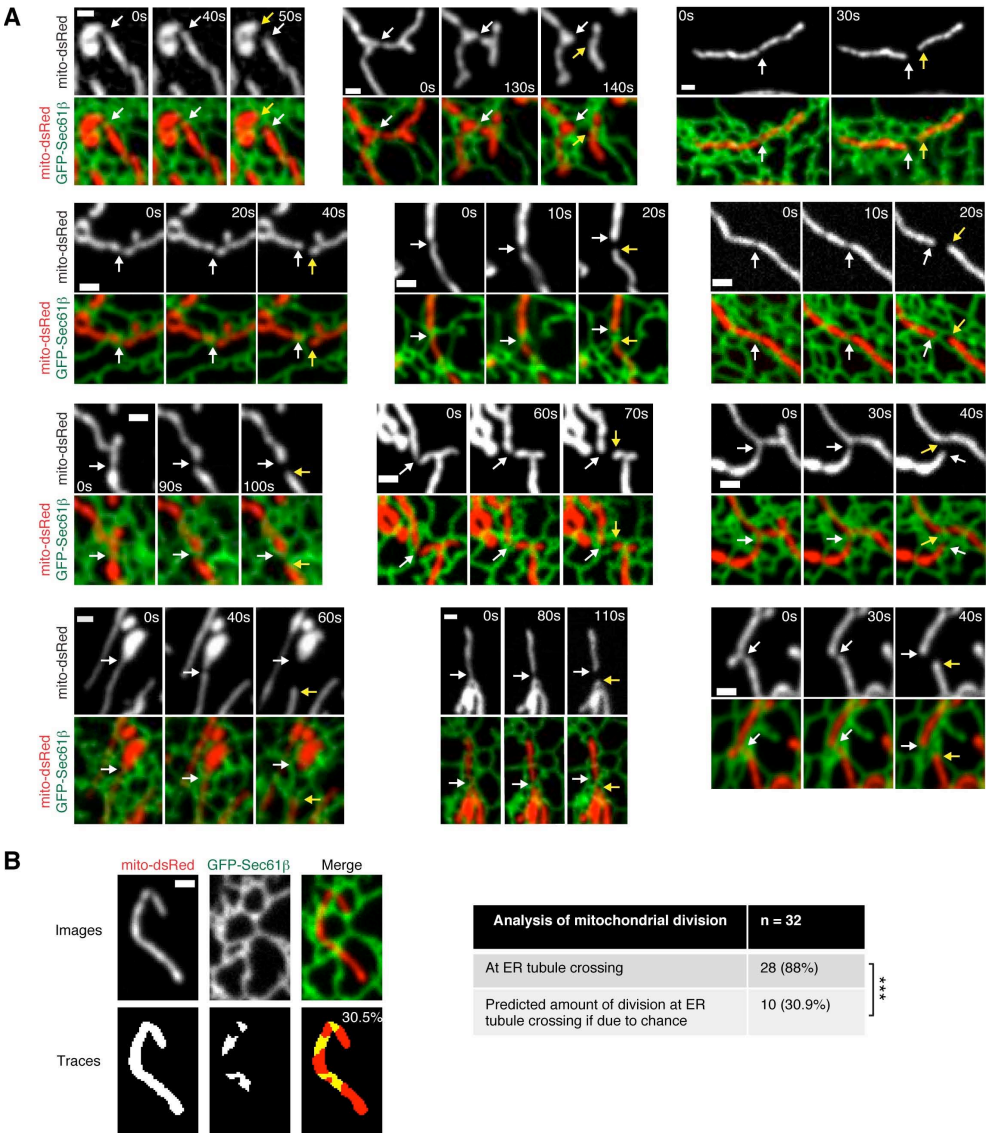

Figure S2. Mitochondrial division occurs at ER-mitochondrial contact sites in mammalian cells. (A) Additional examples of mitochondrial division (as in Fig. 2) during indicated timecourses in Cos-7 cells expressing GFP-Sec61β (ER) and mito-dsRed show that division occurs predominantly at positions where an ER tubule crosses over the mitochondria. Arrows mark the position of mitochondrial division (white arrows) and the position of the newly formed mitochondrial ends (yellow arrows). (B) Method for determining the amount of mitochondrial image surface covered by ER tubule crossing for all 32 division events analyzed. Left panel is an example of mitochondrial and ER tracing from an image immediately preceding mitochondrial fission. Top row shows indicated fluorescence markers and bottom row shows tracings. The percentage shown is the amount of mitochondrial pixels co-localized with pixels from ER tubules crossing the mitochondrion. The right panel table indicates the number of division events at ER-mitochondrial contact sites compared to the expected number of divisions at ER contact if there is no relationship between ER and mitochondrial division (predicted from the percent of the mitochondria covered by crossing ER tubules for all examples). ***, $P<0.0001$, Fisher's exact test. Scale bars: 1 μm.

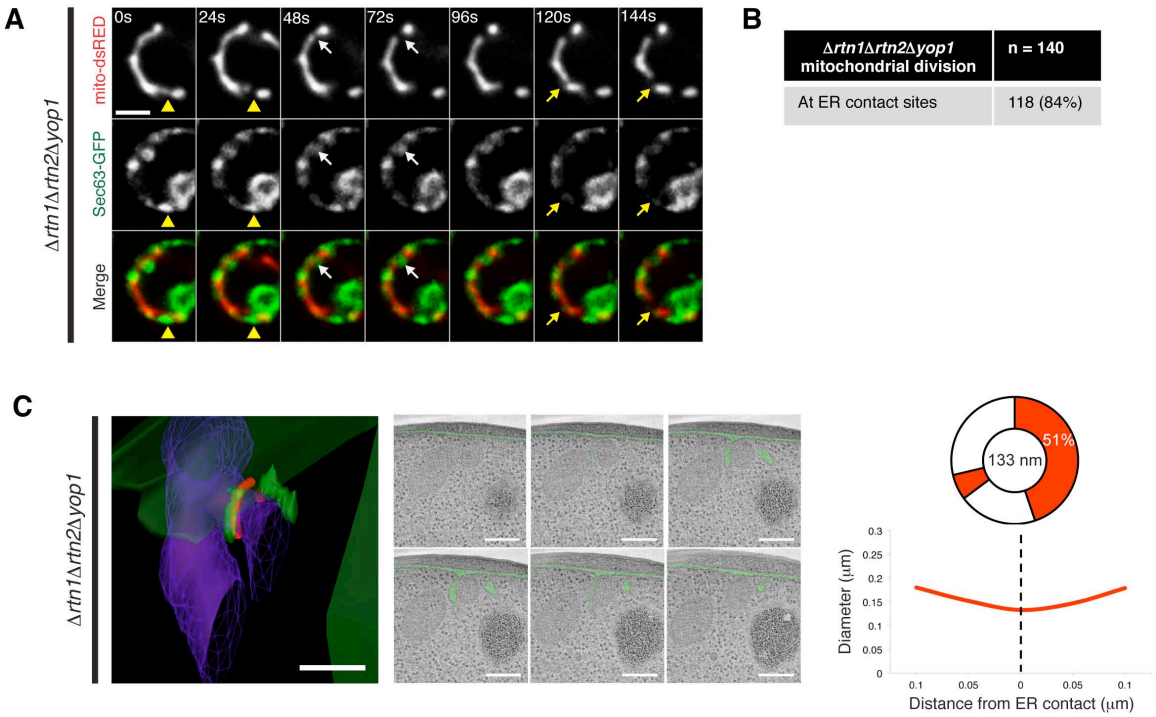

Figure S3. ER tubule-mediated constriction of mitochondria and division occurs at ER contacts in yeast cells without Rtns/Yop1. (A) ER is present at the site of mitochondrial division in the absence of the Rtns/Yop1. Time-lapse images of Δ*rtn1*Δ*rtn2*Δ*yop1* yeast cells expressing mito-dsRED and Sec63-GFP (ER). A single focal plane is shown. Arrows indicate sites of mitochondrial division. (B) Table indicating frequency of mitochondrial division at ER contact sites from 200 cells as in (A). (C) 3-D model and 2-D tomographs (z-series in 15 nm intervals) from yeast Δ*rtn1*Δ*rtn2*Δ*yop1* strain. The region of the mitochondrial circumference that contacts the ER is outlined in red on model (defined as <30 nm distance and ribosome-excluded). Diagram in right panel shows mitochondrial diameter and percent of circumference contacting ER. Right panel graph depicts diameter as in Fig. S1B. Scale bars: (A) 2 μm; (C) 200 nm.

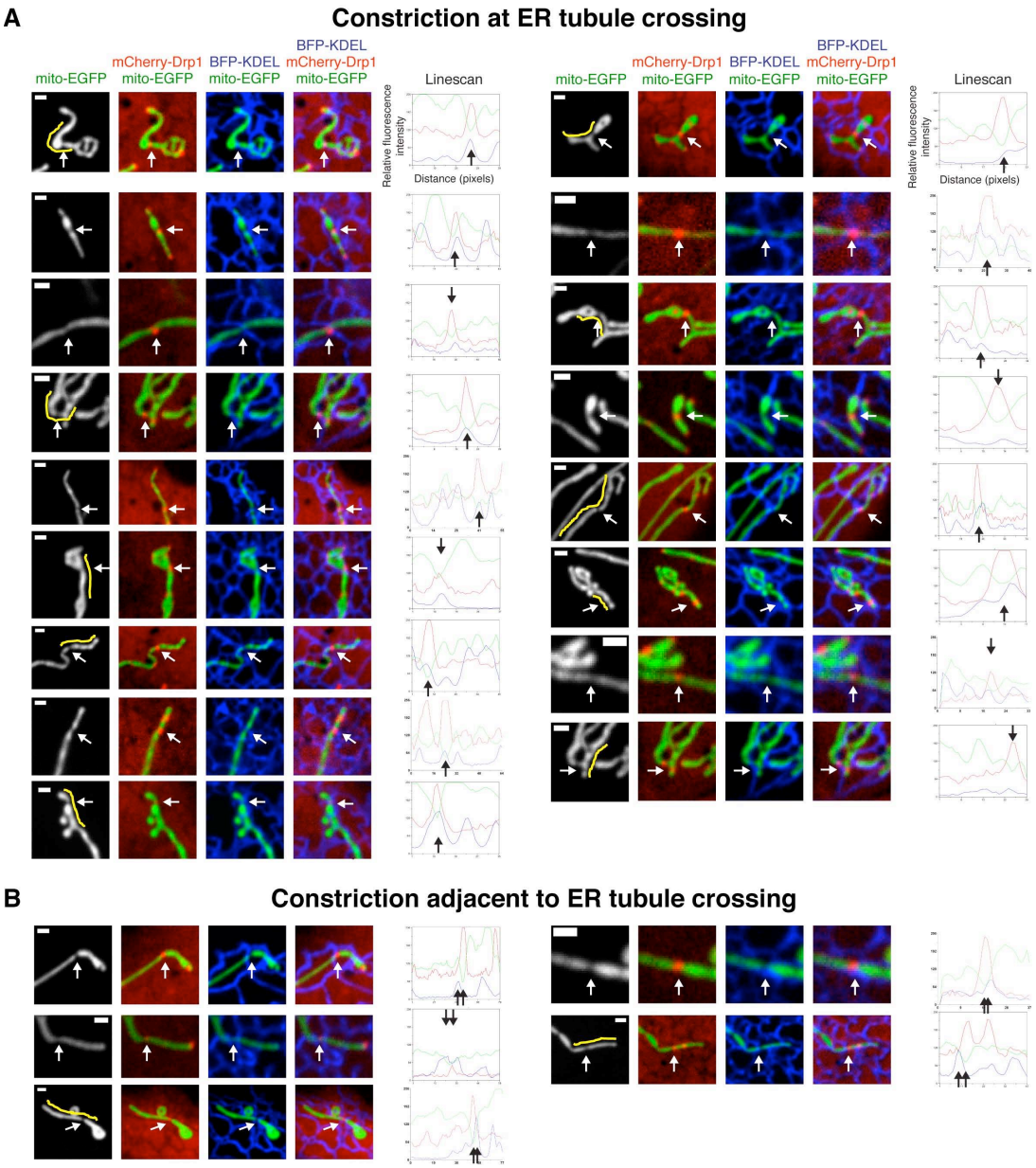

Figure S4. Mitochondrial constrictions at Drp1 punctae are crossed by ER tubules at or near the constriction. (A) Additional examples (as in Fig. 3E) are shown where mitochondrial constriction at the site of Drp1 localization is crossed by an ER tubule. Left panels are images from Cos-7 cells expressing mito-EGFP, BFP-KDEL (ER), and mCherry-Drp1, merged as indicated. Images were taken from the most focused plane of a z-series with a mitochondrial constriction consistent throughout multiple planes. Right panels are Linescans drawn through the mitochondria and show the relative fluorescence intensity of mitochondria (green), ER (blue) and Drp1 (red) along its length. Yellow lines on the mito-EGFP image indicate a Linescan was performed for only that portion of the mitochondrion. White arrows at constrictions on images correspond to black arrows shown on the Linescan. (B) Examples are shown where the constriction is immediately adjacent to an ER tubule crossing. All examples from Fig. 3E and this figure come from a total of 19 cells. Scale bars: 1 μm.

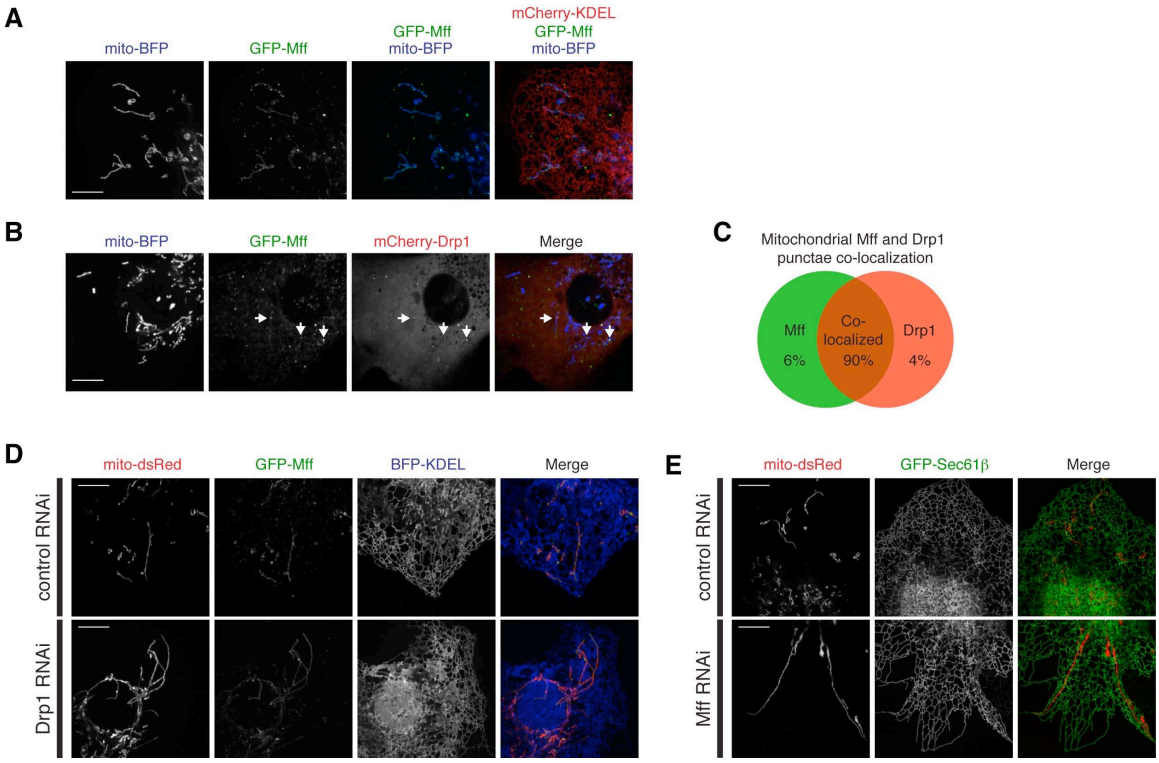

Figure S5. Mff and Drp1 co-localize at mitochondrial punctae and are both required for mitochondrial division in Cos-7 cells. (A) Tagged Mff localizes to mitochondrial punctae. Images are shown from Cos-7 cells expressing GFP-Mff, mito-BFP, and mCherry-KDEL (ER). (B) Tagged Mff and Drp1 co-localize on mitochondria. Images are shown from Cos-7 cells expressing GFP-Mff, mito-BFP, and mCherry-Drp1. Arrows depict co-localized Mff and Drp1 punctae. (C) Chart indicating the co-localization between mitochondrial Mff punctae and mitochondrial Drp1 punctae. 154 punctae were counted from 5 cells that were transfected as in (B). (D) Mff localizes to punctae on elongated mitochondrial networks in the absence of Drp1. Images from Cos-7 cells depleted of Drp1 by RNAi and transfected with GFP-Mff, mito-dsRed, and BFP-KDEL (ER), as in Fig. 4A. (E) Mitochondria are elongated and ER morphology appears normal in Cos-7 cells depleted of Mff by RNAi and transfected with GFP-Sec61β (ER) and mito-dsRed, as in Fig. 4D. Scale bars: 10 μm.

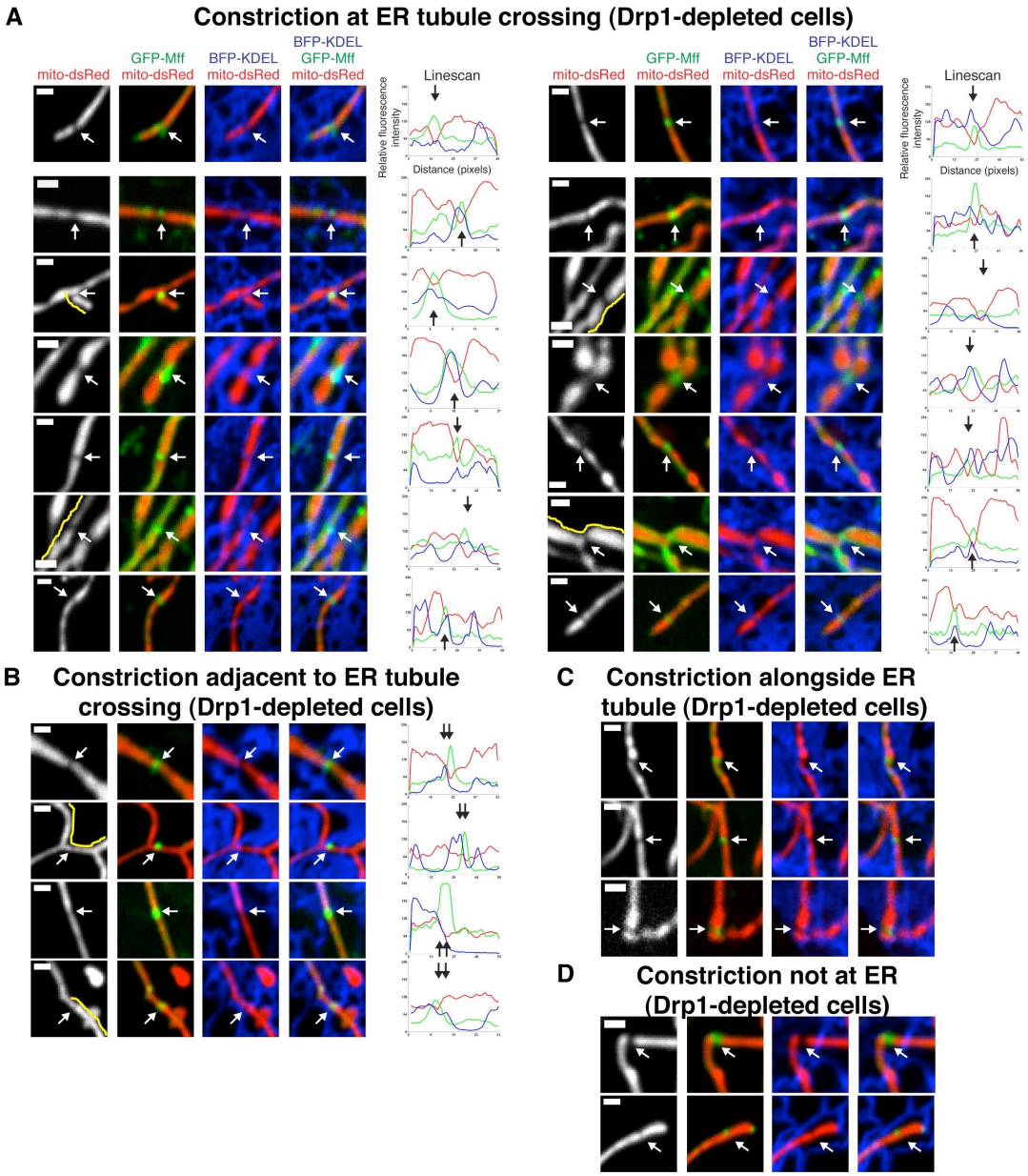

Figure S6. Mitochondrial constrictions correlate with ER-mitochondrial contact sites in Drp1-depleted cells. (A) Additional examples (as in Fig. 4A) are shown where mitochondrial constriction at sites of Mff localization are crossed by an ER tubule. Left panels are images from Drp1-depleted Cos-7 cells expressing mito-dsRed, BFP-KDEL (ER), and GFP-Mff, merged as indicated. Right panels are Linescans drawn through the mitochondria and show the relative fluorescence intensity of mitochondria (red), ER (blue) and Mff (green) along its length. Yellow lines on the mito-dsRed image indicate a Linescan was performed for only that portion of the mitochondrion. White arrows at constrictions on images correspond to black arrows shown on the Linescan. (B) Examples are shown where constriction is immediately adjacent to an ER tubule crossing. (C) Examples are shown where an ER tubule is alongside, but does not cross, a mitochondrial constriction. (D) Examples are shown where the ER does not localize to a mitochondrial constriction. Scale bars: 1 μm.

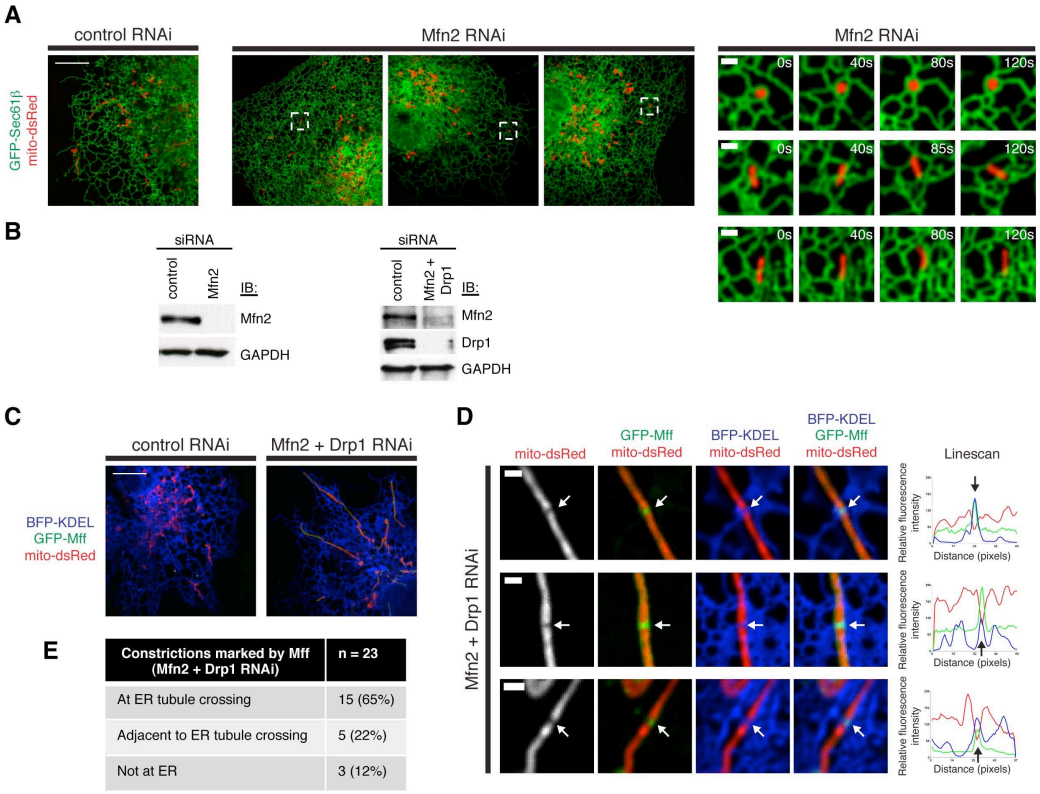

Figure S7. ER-mitochondrial contact at constriction sites persists in cells depleted of the ER-mitochondrial tether, Mfn2. (A) Mitochondria are more fragmented, but maintain ER contact over time in the absence of Mfn2. Images of control (left panel) and Mfn2 RNAi-depleted (center panels) Cos-7 cells expressing GFP-Sec61β (ER) and mito-dsRed. Right panels show zoomed images of regions within dashed boxes on the Mfn2 RNAi cells. The timecourse shown for the zoomed images demonstrates that the fragmented mitochondria are maintaining contact with ER over time at the resolution of light microscopy. (B) Western blots indicating depletion of Mfn2 alone (left panel) or both Mfn2 and Drp1 (right panel) from cells transfected with siRNAs targeted against each protein. Left panel corresponds to cells shown in (A) and right panel corresponds to (C-D). (C) Images of cells depleted of both Mfn2 and Drp1 frequently have elongated mitochondria. Cells shown are transfected with either control siRNA or siRNAs targeted against Mfn2 and Drp1, along with constructs expressing BFP-KDEL (ER), mito-dsRed, and GFP-Mff. (D) Examples of mitochondrial constriction marked by Mff in cells depleted of Mfn2 and Drp1. Left panels are images from Mfn2 and Drp1-depleted cells as in (C), merged as indicated. Right panels are Linescans drawn through the mitochondria and show the relative fluorescence intensity of mitochondria (red), ER (blue) and Mff (green) along its length. White arrows at constrictions on images correspond to black arrows shown on the Linescan. (E) Table indicating the number of Mff-localized mitochondrial constrictions in cells depleted of Mfn2 and Drp1 that co-localize with ER tubules, from 15 cells. Note that constrictions marked by Mff punctae are found at ER tubule crossings at a similar frequency to cells expressing Mfn2 (see Fig. 4C), suggesting Mfn2 does not regulate ER contact at mitochondrial division sites. Scale bars: (left two panels of A, C) 10 μm; (right panel of A, D) 1 μm.

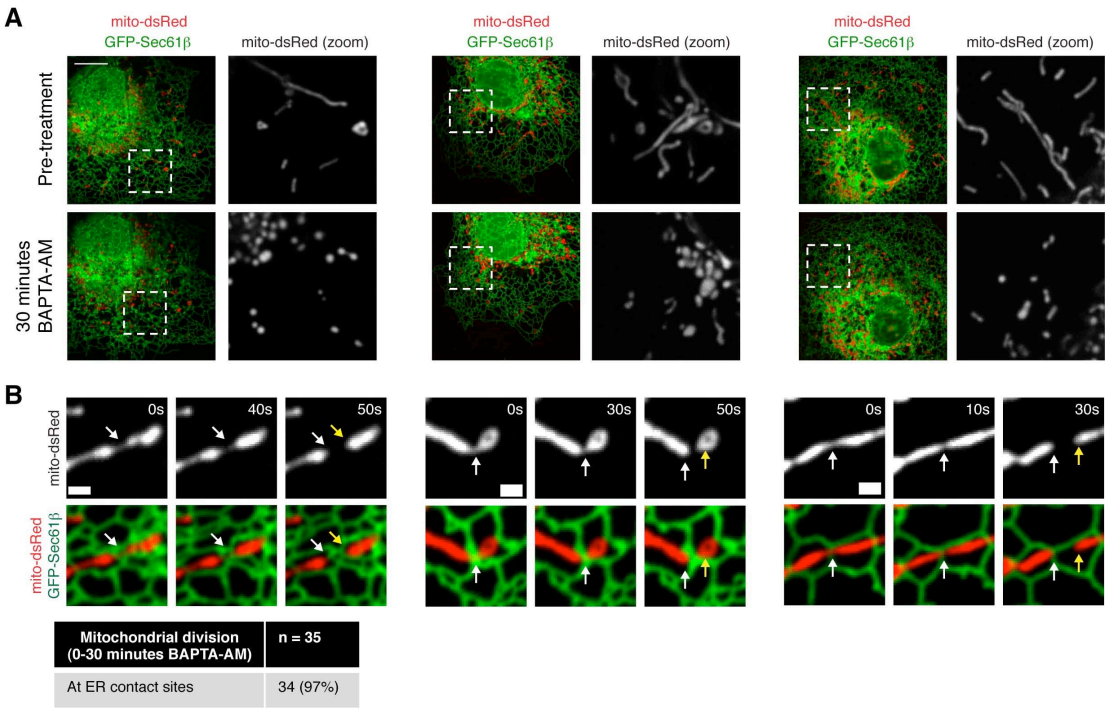

Figure S8. Chelation of cytosolic Ca^{2+} with BAPTA-AM induces mitochondrial division at ER contact sites in a Drp1-dependent manner. (A) Cytosolic Ca^{2+} chelation leads to extensive mitochondrial division within 30 minutes. Images of Cos-7 cells expressing GFP-Sec61β (ER) and mito-dsRed before (top row) and 30 minutes after (bottom row) 10 μM BAPTA-AM treatment. Dashed boxes on left images correspond to zoomed images on right. (B) Mitochondrial division induced upon BAPTA-AM treatment occurs predominantly at ER contacts. Three examples are shown of mitochondrial division events that occur at ER contacts within 30 minutes of treatment of cells as in (A). White arrows indicate the position of mitochondrial division sites and yellow arrows indicate the position of the newly formed mitochondrial ends. Bottom panel is a table indicating the percent of BAPTA-AM induced mitochondrial division events that occur at ER contacts (taken from 7 cells within 30 minutes of treatment). (C) BAPTA-AM induced mitochondrial division at ER contacts is Drp1-dependent. Images shown as in (A) for cells transfected with siRNA targeted against Drp1 (right panel) compared to control siRNA (left panel). Scale bars: (A, C) 10 μm; (B) 1 μm.

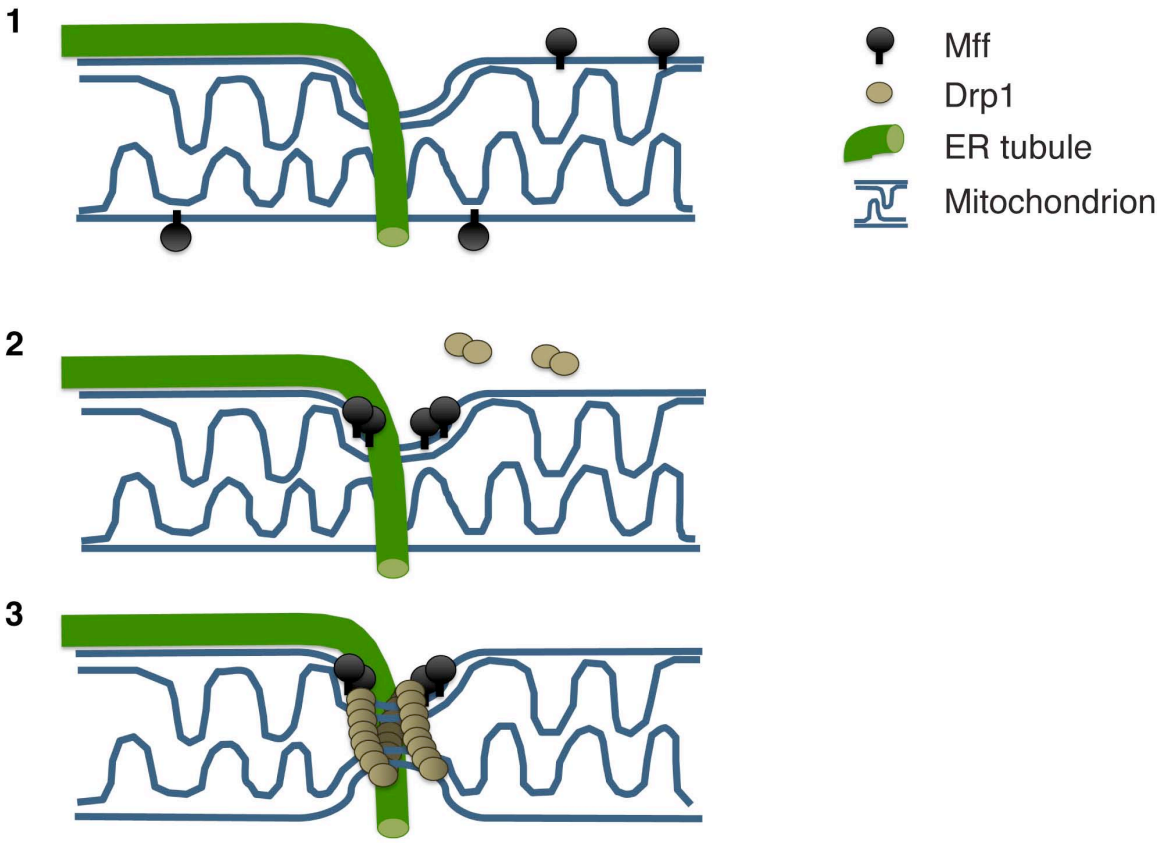

Figure S9. A model for the role of ER in mitochondrial division. (1) An ER tubule associates with and generates a mitochondrial constriction site via unknown factors and/or by physical deformation. (2) In mammalian cells, Mff is recruited to constriction sites in a Drp1-independent manner and (3) Drp1 is then recruited to this site of ER-mitochondrial contact, where the reduced mitochondrial diameter facilitates its assembly into helical structures that subsequently drive fission of the mitochondrial membranes.

Movie S1

3-D reconstruction of ER-mitochondrial contacts in a yeast cell (from Fig. 1A and Fig. S1A, examples a-b). Red object between ER and mitochondria indicates regions of contact that are within 30 nm and are ribosome-excluded. Scale bars = 200 nm.

Movie S2

3-D reconstruction of ER-mitochondrial contacts in a yeast cell (from Fig. 1A and Fig. S1A, examples c-d). Red object between ER and mitochondria indicates regions of contact that are within 30 nm and are ribosome-excluded. Scale bars = 200 nm.

Movie S3

Example of mitochondrial division at a site of ER tubule crossing in a Cos-7 cell expressing GFP-Sec61β (ER) and mito-dsRed. Images of the mitochondria alone (top) are synchronized with images of ER and mitochondria merged (bottom). Example is from Fig. 2A. Images were taken every 10 seconds, and are shown at 2 frames per second.

Movie S4

Example of mitochondrial division at a site of ER tubule crossing in a Cos-7 cell expressing GFP-Sec61β (ER) and mito-dsRed. Images of the mitochondria alone (top) are synchronized with images of ER and mitochondria merged (bottom). Example is from Fig. 2D. Images were taken every 10 seconds, and are shown at 2 frames per second.

Movie S5

Drp1 punctae localize to ER-mitochondrial contacts over time in Cos-7 cells. Example is from a cell expressing mito-BFP, GFP-Sec61β (ER), and mCherry-Drp1. Images were taken every 5 seconds for 2 minutes, and are shown at 6 frames per second.